fluorescence optics. The DiI-injected embryos were fixed in 4% paraformaldehyde, embedded in polyester wax, sectioned at 10 μm, and sections were viewed unstained with bright-field and fluorescence optics.

HNK-1 staining

Larvae were fixed in 4% paraformaldedyde in PBS for 30 min at room temperature and then in 100% methanol for 5 min at −20 °C. The fixed larvae were washed in PBS containing 1% Triton X-100, and stained with a 1:20 dilution of HNK-1 antibody (Biopharmagen) for 24 h at 4 °C using the Vectastain ABC Peroxidase kit (Vector Laboratories). Antibody incubations and blocking were carried out in 2% Superblock and controls used non-immune mouse serum.

EtZic isolation and *in situ* hybridization

The oligodexoynucleotide primers AARGCMAAATACAARCTRATCAACC (forward) and ACYTTCATGTGCTTSCKRAGRGAGC (reverse) were used to isolate part of an *Ecteinascidia Zic* gene by polymerase chain reaction with reverse transcription (RT–PCR) from total larval RNA. BLAST searches and tree building suggested that *EtZic* is most closely related to *CsZicr2* (ref. 21), *AmphiZic* (ref. 22), and the vertebrate *Zic2* (refs 18–20) genes. *In situ* hybridization with a digoxygenin-labelled probe was carried out as described previously[30].

Received 23 July; accepted 25 August 2004; doi:10.1038/nature02975.

1. Hall, B. K. *The Neural Crest in Development and Evolution* (Springer, New York, 1999).
2. Le Douarin, N. & Kalcheim, C. *The Neural Crest* 2nd edn (Cambridge Univ., Cambridge, 1999).
3. Baker, C. V. H. & Bronner-Fraser, M. The origins of the neural crest. Part II: an evolutionary perspective. *Mech. Dev.* **69,** 13–29 (1997).
4. Gans, C. & Northcutt, R. G. Neural crest and the origin of vertebrates: a new head. *Science* **220,** 268–274 (1983).
5. Shimeld, S. M. & Holland, P. W. H. Vertebrate innovations. *Proc. Natl Acad. Sci. USA* **97,** 4449–4452 (2000).
6. Wada, H. Origin and evolution of the neural crest: A hypothetical reconstruction of its evolutionary history. *Dev. Growth Diff.* **43,** 509–520 (2001).
7. Stone, J. R. & Hall, B. K. Latent homologues of the neural crest as an evolutionary novelty. *Evol. Dev.* **6,** 123–129 (2004).
8. Corbo, J. C., Erives, A., DiGregorio, A. & Levine, M. Dorsoventral patterning of the vertebrate neural tube is conserved in a protochordate. *Development* **124,** 2335–2344 (1997).
9. Langeland, J. A., Tomsa, J. M., Jackman, W. R. & Kimmel, C. B. An amphioxus snail gene: Expression in paraxial mesoderm and neural plate suggests a conserved role in patterning the chordate embryo. *Dev. Genes Evol.* **208,** 569–577 (1998).
10. Holland, L. Z. & Holland, N. D. Evolution of the neural crest and placodes: amphioxus as a model system. *J. Anat.* **199,** 85–98 (2001).
11. Jeffery, W. R. & Swalla, B. J. Evolution of alternate modes of development in ascidians. *BioEssays* **14,** 219–226 (1992).
12. Berrill, N. J. Studies in tunicate development. III. Differential retardation and acceleration. *Phil. Trans. R. Soc. Lond. B* **225,** 255–326 (1935).
13. Lyerla, T. A., Lyerla, J. H. & Fisher, M. Pigmentation in the orange tunicate *Ecteinascidia turbinata*. *Biol. Bull.* **149,** 178–185 (1975).
14. Thiery, J.-P., Duband, J. L. & Dolouvée, A. Pathways and mechanisms of avian trunk neural crest cell migration and localization. *Dev. Biol.* **93,** 324–343 (1982).
15. Jungalwala, F. B., Chou, D. K. H., Suzuki, Y. & Maxwell, G. D. Temporal expression of HNK-1 reactive sulfoglucuronyl glycolipid in cultured quail trunk neural crest cells—comparison with other developmental regulated glycolipids. *J. Neurochem.* **58,** 1045–1051 (1992).
16. Akitaya, T. & Bronner-Fraser, M. Expression of cell adhesion molecules during initiation and cessation of neural crest cell migration. *Dev. Dyn.* **194,** 12–20 (1992).
17. Hirata, M., Ito, K. & Tsuneki, K. Migration and colonization patterns of HNK-1 immunoreactive neural crest cells in lamprey and swordfish embryos. *Zool. Sci.* **14,** 305–312 (1997).
18. Nakata, K., Nagai, T., Aruga, J. & Mikoshiba, K. *Xenopus* Zic family and its role in neural and neural crest development. *Mech. Dev.* **75,** 43–51 (1998).
19. Brewster, R., Lee, J. & Ruiz i Altaba, A. Gli/Zic factors pattern the neural plate by determining domains of cell differentiation. *Nature* **398,** 579–583 (1998).
20. Elms, P., Siggers, P., Napper, D., Greenfield, A. & Arkell, R. Zic2 is required for neural crest formation and hindbrain patterning during mouse development. *Dev. Biol.* **264,** 391–406 (2003).
21. Atou, Y. *et al.* macho-1 related genes in *Ciona* embryos. *Dev. Genes Evol.* **212,** 87–92 (2002).
22. Gostling, N. J. & Shimeld, S. M. Protochordate Zic genes define primitive compartments and highlight molecular changes underlying neural crest evolution. *Evol. Dev.* **5,** 136–144 (2003).
23. Katz, M. J. Comparative anatomy of the tunicate tadpole *Ciona intestinalis*. *Biol. Bull.* **164,** 1–27 (1983).
24. Wada, H., Saiga, H., Satoh, N. & Holland, P. W. H. Tripartite organization of the ancestral chordate brain and the antiquity of the placodes: Insights from ascidian Pax-2/5/8, Hox, and Otx genes. *Development* **125,** 1113–1122 (1998).
25. Erickson, C. A. From the crest to the periphery: Control of pigment cell migration and lineage segregation. *Pigment. Cell Res.* **6,** 336–347 (1993).
26. Burighel, P., Lane, N. J., Zaniolo, G. & Manni, L. The neurogenic role of the neural gland in the development of the ascidian *Botryllus schlosseri* (Tunicata, Ascidiacea). *J. Comp. Neurol.* **394,** 230–241 (1998).
27. Manni, L., Lane, N. J., Sorrentino, M., Zaniolo, G. & Burighel, P. Mechanisms of neurogenesis during the embryonic development of a tunicate. *J. Comp. Neurol.* **412,** 527–541 (1999).
28. Manni, L., Lane, N. J., Burighel, P. & Zaniolo, G. Are neural crest and placodes exclusive to the vertebrates? *Evol. Dev.* **3,** 297–298 (2001).
29. Thorndyke, M. C. & Probert, L. Calcitonin-like cells in the pharynx of the ascidian *Styela clava*. *Cell Tissue Res.* **203,** 301–309 (1979).
30. Olsen, C. L. & Jeffery, W. R. A *forkhead* gene related to *HNF-3β* is required for gastrulation and axis formation in the ascidian embryo. *Development* **124,** 3609–3619 (1997).

Acknowledgements This work was supported by grants to W.R.J. from the National Science Foundation, the National Institutes of Health, and the Bermuda Biological Station. We thank D. Martasian, A. Parkhurst, and L. Reed for technical assistance.

Competing interests statement The authors declare that they have no competing financial interests.

Correspondence and requests for materials should be addressed to W.R.J. (jeffery@umd.edu). The EtZic DNA sequence has been deposited in GenBank under accession number AY176563.

Role for a cortical input to hippocampal area CA1 in the consolidation of a long-term memory

Miguel Remondes & Erin M. Schuman

Caltech/HHMI, Division of Biology, 114-96, Pasadena, California 91125, USA

A dialogue between the hippocampus and the neocortex is thought to underlie the formation, consolidation and retrieval of episodic memories[1–4], although the nature of this cortico-hippocampal communication is poorly understood. Using selective electrolytic lesions in rats, here we examined the role of the direct entorhinal projection (temporoammonic, TA) to the hippocampal area CA1 in short-term (24 hours) and long-term (four weeks) spatial memory in the Morris water maze. When short-term memory was examined, both sham- and TA-lesioned animals showed a significant preference for the target quadrant. When re-tested four weeks later, sham-lesioned animals exhibited long-term memory; in contrast, the TA-lesioned animals no longer showed target quadrant preference. Many long-lasting memories require a process called consolidation, which involves the exchange of information between the cortex and hippocampus[3,5,6]. The disruption of long-term memory by the TA lesion could reflect a requirement for TA input during either the acquisition or consolidation of long-term memory. To distinguish between these possibilities, we trained animals, verified their spatial memory 24 hours later, and then subjected trained animals to TA lesions. TA-lesioned animals still exhibited a deficit in long-term memory, indicating a disruption of consolidation. Animals in which the TA lesion was delayed by three weeks, however, showed a significant preference for the target quadrant, indicating that the memory had already been adequately consolidated at the time of the delayed lesion. These results indicate that, after learning, ongoing cortical input conveyed by the TA path is required to consolidate long-term spatial memory.

To assess the role of the TA pathway in the acquisition and retention of spatial memory in the rat, we identified stereotaxic coordinates to target the TA axons for electrolytic ablation. We used histology, electrophysiology, and retrograde tracing techniques to verify the extent and specificity of the TA lesions. We included in our behavioural analysis data from animals with relatively restricted lesions in the stratum lacunosum moleculare, the region where TA axons terminate in area CA1 (Fig. 1a,b and Supplementary Figs 1 and 2); we excluded animals in which the lesion extended significantly into the perforant path input to the dentate gyrus. We performed electrophysiological recordings on a subset of slices, and assessed synaptic transmission in the perforant path–dentate gyrus, TA–CA1 and CA1–subiculum pathways with extracellular stimulation and recordings (Fig. 1c). Brain slices from sham-lesioned animals showed normal synaptic transmission at all three sets of synapses (Fig. 1c). Slices from TA-lesioned animals exhibited

normal synaptic transmission at the perforant path–dentate gyrus and CA1–subiculum synapses, but a complete loss of synaptic responses at the TA–CA1 synapse (Fig. 1c). The TA axons originate in entorhinal cortex (EC) layer III and the trisynaptic pathway originates in EC layer II. Thus, using a unique set of coordinates, we injected a fluorescence-labelled retrograde tracer (cholera toxin subunit B) targeting both the dentate gyrus and CA1 and examined the distribution of fluorescence in the EC layers (Fig. 1d). Sham-lesioned animals exhibited significant fluorescence labelling in both layers II and III, whereas TA-lesioned animals exhibited significant labelling in layer II only (Fig. 1d). Taken together, these data indicate that we achieved a restricted ablation of TA input to CA1 without significant damage to the parallel trisynaptic circuit.

We tested the ability of the TA-lesioned rats to acquire, retain, consolidate and retrieve spatial information in the Morris water maze[1], comparing the performance of sham-, TA- and hippocampal-lesioned animals (Fig. 2a). Animals that received lesions did not differ significantly from sham-lesioned animals in their ability to navigate towards a visible platform (Supplementary Fig. 3). As shown by others, the complete ablation of the hippocampus prior to training resulted in significant learning impairments[1], as indicated by longer latencies (Fig. 2b) and reduced target quadrant preference during probe trials (Supplementary Fig. 3b). In contrast, animals that received lesions restricted to the TA path showed immediate and short-term (24-h) spatial learning that was indistinguishable from sham-lesioned controls (Fig. 2c). Taken together with the anatomical data (Fig. 1), these data suggest that the hippocampal output is not substantially affected in the TA-lesioned animals. This result indicates that the TA input to the hippocampus is not required for rats to learn the platform location or for short-term memory.

Memories can be transformed from labile (short-term) to a relatively stable (long-term) form by a process referred to as consolidation. Some theories of long-term memory posit that following initial learning, a prolonged interaction between hippocampal and cortical circuits is required to consolidate the memory at the 'systems' level[3,5,6]. We reasoned that the TA input might be important for these post-training cortico-hippocampal interactions. We first tested whether control animals exhibited long-term memory, assessed four weeks after training, for the target quadrant. In the absence of any additional (for example, beyond 24 h) exposure to the pool, sham-lesioned animals exhibited significant preference for the target quadrant four weeks after training (Fig. 2d), indicating that our training protocol is sufficient to

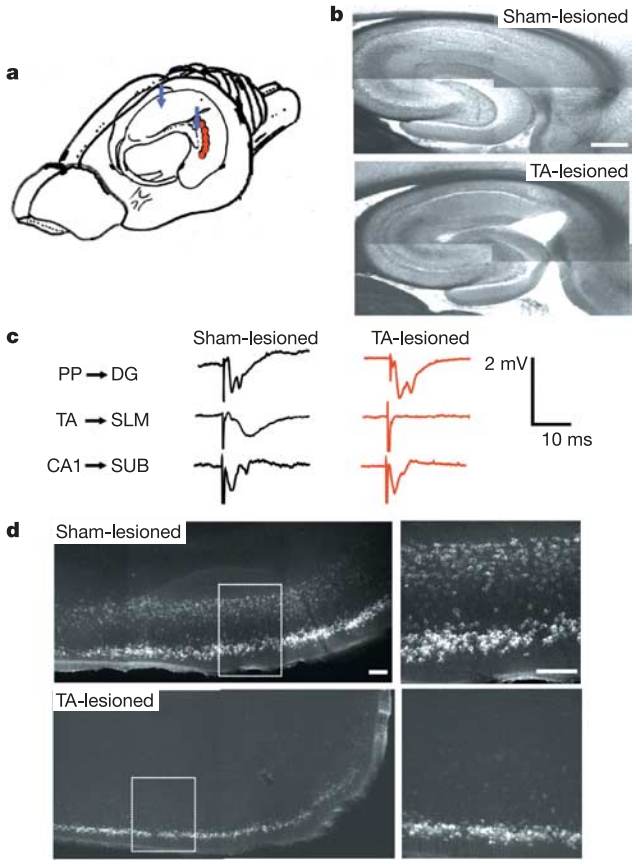

Figure 1 Specificity of TA lesions. **a**, Rat brain hippocampal formation with electrolytic lesion sites[15,17,18] shown in red. **b**, Representative sections from sham- and TA-lesioned animals. Scale bar, 250 μm. See also Supplementary Figs 1 and 2. **c**, Representative field potential recordings from hippocampal slices prepared from sham- or TA-lesioned animals. PP, perforant path; DG, dentate gyrus; SLM, stratum lacunosum moleculare; SUB, subiculum. **d**, Representative images of entorhinal cells labelled by the fluorescent retrograde tracer (injection positions shown by blue arrows in **a**). In sham-lesioned animals the tracer labelled cells in layers II and III. In TA-lesioned animals the labelling was largely confined to layer II. Scale bar, 100 μm.

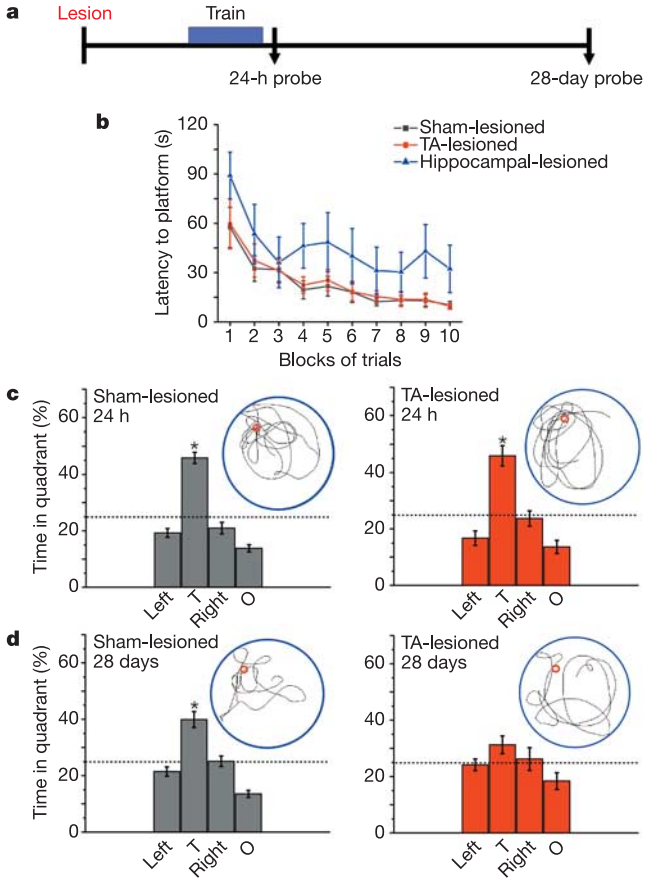

Figure 2 TA-lesioned animals exhibit deficits in long-term, but not short-term spatial memory. **a**, Experiment time-line. **b**, Mean escape latencies for sham-lesioned ($n = 21$), hippocampal-lesioned ($n = 5$) and TA-lesioned groups ($n = 10$). **c**, Mean time that each group spent in indicated quadrants during a short-term memory probe trial (24 h after training ended). Quadrants are left, T (target), right and O (opposite to target). Both groups showed a significant preference ($P \leq 0.05$) for the target quadrant. Error bars depict the standard error of the mean, s.e.m. Insets are a representative swim path from a single animal during a probe trial. **d**, Mean time that each group spent in each quadrant during a long-term memory probe trial (28 days after training ended). Sham-lesioned animals (15/21) still showed a significant preference for the target ($P \leq 0.05$) whereas, on average, TA-lesioned animals (4/10) no longer showed significant memory for the target.

produce both short-term (24 h) and long-term (four weeks) memory. Surprisingly, the TA-lesioned animals that exhibited significant target preference when tested after 24 h lost their memory for the target quadrant when tested four weeks after training (Fig. 2d). Taken together, these data indicate that TA lesions selectively affect long-term (~1 month) memory, without affecting short-term (~24 h) memory. These results suggest that the TA input to area CA1 is required for the establishment of a long-term spatial memory.

The disruption of long-term memory by the TA lesion could reflect a requirement for TA input to acquire long-term memory, or, alternatively, could reflect a requirement for TA-conveyed cortical input to consolidate a long-term spatial memory. To distinguish between these two possibilities, we lesioned the TA pathway after training and testing animals for short-term (24 h) memory (Fig. 3a). Before the administration of lesions, all animals learned the platform location at the same rate (Fig. 3b). In addition, both the sham- and future TA-lesioned animals showed significant preference for the target quadrant when examined 24 h after the end of training (Fig. 3c). Trained animals then received either a sham or a TA lesion; four weeks later, their preference for target quadrant was re-assessed. Sham-lesioned animals still exhibited a significant preference for the target quadrant (Fig. 3d). TA-lesioned animals, however, no longer showed memory for the target quadrant (Fig. 3d). Because the lesion was administered after successful learning and short-term memory, the impaired performance of the lesioned animals indicates an ongoing requirement for TA input for the consolidation and/or retrieval of a long-term spatial memory, rather than its acquisition.

If the TA-conveyed cortical activity is required for consolidation of memory then a finite window of vulnerability to perturbation is predicted. To address this, we conducted an additional set of experiments in which the TA lesion was executed three weeks after learning; sham- and TA-lesioned animals were then given a final probe trial at 30 days (Fig. 4a). As before, prior to the administration of lesions, all animals learned the platform location at the same rate (Fig. 4b). In addition, both the sham- and future TA-lesioned animals showed a significant preference for the target quadrant when examined 24 h after the end of training (Supplementary Fig. 3c). Three weeks later, another probe trial was conducted and a randomly selected subset of the animals that exhibited significant target quadrant preference (Fig. 4c) received TA lesions. Nine days later (on day 30), a final probe trial revealed that both the sham- and the TA-lesioned animals exhibited a

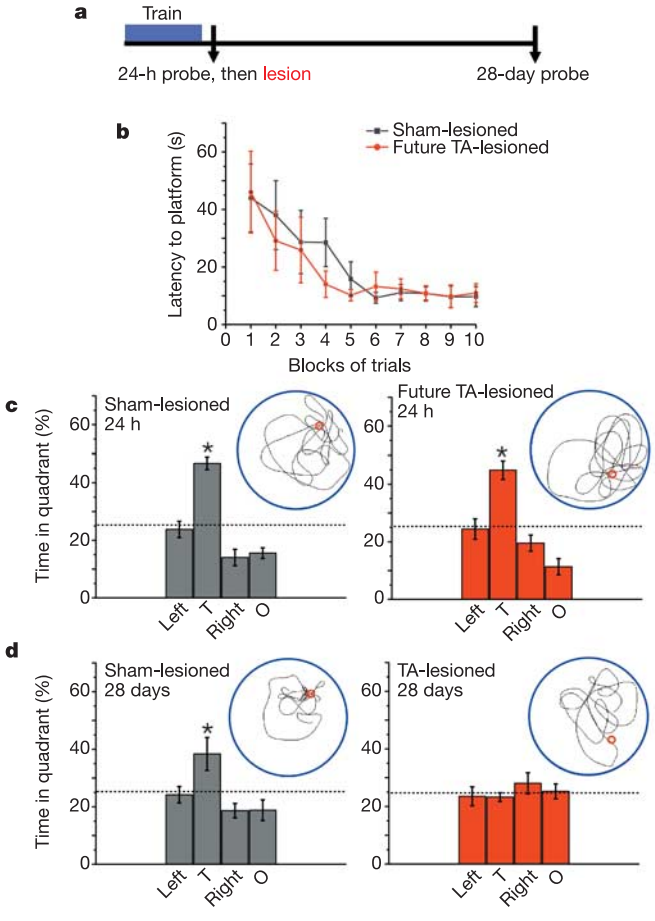

Figure 3 Disruption of the TA path 24 h after learning resulted in deficits in long-term spatial memory. **a**, Experiment time-line. **b**, Mean escape latencies for the sham-lesioned ($n = 8$) and future TA-lesioned ($n = 8$) groups, which showed similar learning rates. **c**, Mean time that the each group spent in indicated quadrant during a short-term memory probe trial. Both groups showed a significant preference ($P \leq 0.5$) for the target quadrant. **d**, Mean time that each group spent in each quadrant during a long-term memory probe trial. Sham-lesioned animals (7/8) still showed a significant preference for the target quadrant ($P \leq 0.05$), whereas the TA-lesioned animals (0/8) no longer exhibited memory for the trained location. The groups differed significantly in their target preference ($P \leq 0.05$).

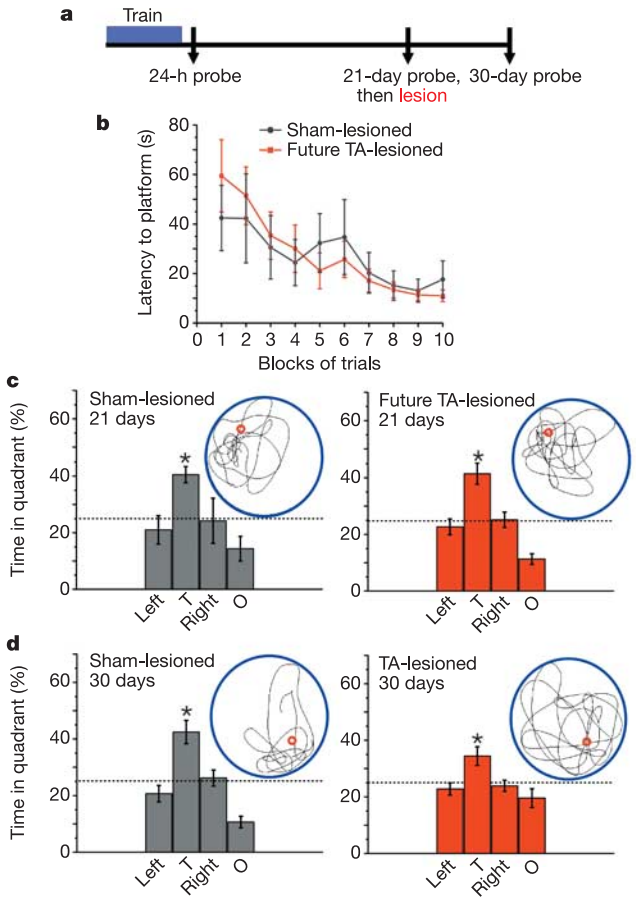

Figure 4 Disruption of the TA path three weeks after learning does not abolish long-term spatial memory. **a**, Experiment time-line. **b**, Mean escape latencies for the sham-lesioned ($n = 6$) and future TA-lesioned ($n = 9$) groups, which showed similar learning rates. **c**, Mean time that each group spent in indicated quadrant during a probe trial conducted 21 days after training. Both groups showed a significant preference ($P \leq 0.05$) for the target. **d**, Mean time that sham- or TA-lesioned animals spent in each quadrant during a long-term memory probe trial. Both sham-lesioned (6/6) and TA-lesioned animals (7/9) showed significant preference for the target quadrant ($P \leq 0.05$) and did not differ significantly from one another.

significant preference for the target quadrant relative to the other quadrants (Fig. 4d). Thus, a disruption of the TA input three weeks after learning failed to disrupt the long-term memory for the learned quadrant, whereas a TA disruption within 24 h (Fig. 3) abolished the memory. These results indicate that the temporal window for long-term memory consolidation lasts, on average, less than three weeks following training.

Previous studies have shown that deafferentation[7,8] or ablation[1,9] of the hippocampus disrupts the rate of learning and short-term memory for the platform location in the Morris water maze. Restricted lesions, however, that target individual pathways in the trisynaptic circuit have often resulted in little memory impairment. For example, lesions restricted to the dentate gyrus[10] or area CA3[11,12] do not affect the acquisition of spatial memory tasks[11,12] or the development and stability of place cells in area CA1[10,12]. In addition, mice possessing a conditional deletion of the NMDA receptor in area CA3, which abolishes commissural–CA3 long-term potentiation, show normal acquisition of spatial memory in the standard Morris water maze[13]. Our results suggest that the normal spatial learning exhibited by animals with targeted disruptions of the trisynaptic circuit might be due to information conveyed by the TA input to area CA1.

Recent studies have shown that TA–CA1 synapses exhibit synaptic plasticity, including LTP[14–16] and LTD[17]. Appropriately timed TA bursting can also modulate Schaffer collateral-elicited spiking activity[18] and plasticity[15] in the hippocampal CA1 field. Transmission at the TA–CA1 can also be regulated by neuromodulators[19] that are known to influence spatial memory[20,21]. These observations provide a potential synaptic framework for understanding the regulation of memory consolidation by the TA input.

Thus our data show that animals that received selective lesions of the TA input to the hippocampus exhibited normal learning and short-term spatial memory, but failed to maintain the memory for an extended period of time. In a related experiment, pharmacologic inactivation of the hippocampus either 1–7 or 7–12 days after water maze training disrupted the memory for the target quadrant preference[22]. In addition, mice heterozygous for an α-CAMKII mutation show short-term memory for the target quadrant that decays over a 10–17-day retention period[23]. In our experiments, a long-term memory deficit was evident when the TA input was interrupted before or 24 h after the learning experience, but not when disrupted three weeks after training, suggesting that the consolidation period had ended by this time. The observation that TA-lesioned animals were able to retrieve information about the correct target 24 h after learning, or when the TA-lesion was delayed to 21 days after training, argues against a simple deficit in retrieval. These results indicate that, following learning, ongoing cortical input conveyed by the TA path is required to consolidate long-term spatial memory. Coordinated activity between hippocampal and cortical circuits has been observed during sleep episodes[24,25] often associated with memory consolidation[26,27]. Further research should aim to establish the precise nature and function of the TA-conveyed cortical information during memory consolidation. □

Methods

Standard techniques used for surgical procedures, lesion execution and assessment and electrophysiology are described in the Supplementary Methods.

Animals

All animals used were male adult Long Evans rats (290–340 g; Charles River or Simonsen). Use of animals was performed according to the guidelines of the Caltech Institutional Animal Care and Use Committee.

Morris water maze

A pool 2.0 m in diameter filled with water made opaque with white non-toxic ink (Jazz Gloss Tempera white, Van Aken International) maintained at 25.0 ± 2.0 °C was used. The maze was located in a laboratory room, with distal cues at several locations. After a recovery period of at least ten days after surgery, animals were brought to the behaviour room (where they were housed for the duration of the training), handled for 1–2 days, and trained.

The full protocol consisted of seven days in which the first trial was always a probe trial, that is, there was no platform in the pool, to assess any spatial bias before the initiation of training and to observe the acquisition of quadrant preference during the previous trials. In probe trials, the animal was released from the centre of the pool, with its head facing a different room wall every day; animals were allowed to swim in the pool for 60 s. The quadrant preference was assessed as the percentage of total time rats spent in each of the four quadrants. The first training day consisted of a probe trial followed by a 'visible platform' trial, in which the platform was indicated by a red/orange flag. After this, rats were given their first 'hidden platform' learning trial, during which they were allowed to rest on the platform for 30 s before being released from one of the pool's starting points (north, south, east or west). Animals were allowed 120 s to find the platform and allowed to stay there for 30 s; if animals did not find the platform in 120 s they were picked up from the water and put on the platform for 30 s.

A block of trials consisted of four trials corresponding to four different randomized release points. The subsequent four days consisted of one probe trial followed by two training blocks (a total of eight trials) with at least a two-hour interval between blocks. To compensate for possible extinction resulting from the daily probe trial, the first training block (after the probe trial), and this one only, began with the placement of the rat on the platform for 30 s. On the last training day, a single training block followed the usual probe trial. On the following day animals were given a single probe trial, 24 h after the last learning trial—this is referred to in the text as the 24-h probe. Therefore, the total training took six days followed by the last 24-h probe on the seventh day. The rats were then returned to their home cages and were tested later for long-term memory 28–30 days after the 24-h probe trial. In two different sets of experiments, animals were lesioned either immediately after the 24-h probe trial, or after a 21-day-delay probe trial.

Data were collected by an HVS (UK) system—a charge-coupled device (CCD) camera connected to a PC card inserted in an IBM-compatible laptop computer. Software tracked the successive positions of the rat in the pool at a rate of 10 Hz for the duration of each trial. Data were analysed with the Water 2002 HVS (UK) software, and the summary data were transferred to Microcal Origin for further analysis and graphic display. The data for acquisition and retention were analysed by comparing the quadrant preferences and escape latencies averaged across animals of the same surgical group, using analysis of variance (ANOVA). The water maze probe data were analysed within group and experiment to assess quadrant preference, and later analysed between groups (ANOVA and unpaired *t*-test) to assess differences between quadrant preferences across different surgical and retention time groups. Differences were considered statistically significant at $P < 0.05$.

Received 8 June; accepted 16 August 2004; doi:10.1038/nature02965.

1. Morris, R. G. M., Garrud, P., Rawlins, J. N. P. & O'Keefe, J. Place navigation impaired in rats with hippocampal lesions. *Nature* **297,** 681–683 (1982).
2. Eichenbaum, H. A cortical-hippocampal system for declarative memory. *Nature Rev. Neurosci.* **1,** 41–50 (2001).
3. Scoville, W. B. & Milner, B. Loss of recent memory after bilateral hippocampal lesions. *J. Neuropsychiatry Clin. Neurosci.* **12,** 103–113 (1957).
4. Squire, L. R. & Zola, S. M. Amnesia, memory and brain systems. *Phil. Trans. R. Soc. Lond. B* **352,** 1663–1673 (1997).
5. McGaugh, J. L. Time-dependent processes in memory storage. *Science* **153,** 1351–1358 (1966).
6. Squire, L. R. & Alvarez, P. Retrograde amnesia and memory consolidation: a neurobiological perspective. *Curr. Opin. Neurobiol.* **5,** 169–177 (1995).
7. Skelton, R. W. & McNamara, R. K. Bilateral knife cuts to the perforant path disrupt spatial learning in the Morris water maze. *Hippocampus* **2,** 73–80 (1992).
8. Eichenbaum, H., Stewart, C. & Morris, R. G. M. Hippocampal representation in place learning. *J. Neurosci.* **10,** 3531–3542 (1990).
9. Sutherland, R. J., Whishaw, I. Q. & Kolb, B. A behavioural analysis of spatial localization following electrolytic, kainate- or colchicine-induced damage to the hippocampal formation in the rat. *Behav. Brain Res.* **7,** 133–153 (1983).
10. McNaughton, B. L., Barnes, C. A., Meltzer, J. & Sutherland, R. J. Hippocampal granule cells are necessary for normal spatial learning but not for spatially-selective pyramidal cell discharge. *Exp. Brain Res.* **76,** 485–496 (1989).
11. Jarrard, L. E. Selective hippocampal lesions and behaviour: effects of kainic acid lesions on performance of place and cue tasks. *Behav. Neurosci.* **97,** 873–889 (1983).
12. Brun, V. H. *et al.* Place cells and place recognition maintained by the direct entorhinal-hippocampal circuitry. *Science* **296,** 2243–2246 (2002).
13. Nakazawa, K. *et al.* Requirement for hippocampal CA3 NMDA receptors in associative memory recall. *Science* **297,** 211–218 (2002).
14. Colbert, C. M. & Levy, W. B. Long-term potentiation of perforant path synapses in hippocampal CA1 in vitro. *Brain Res.* **606,** 87–91 (1993).
15. Remondes, M. & Schuman, E. M. Direct cortical input modulates plasticity and spiking in CA1 pyramidal neurons. *Nature* **416,** 736–740 (2002).
16. Remondes, M. & Schuman, E. M. Properties of early- and late-phase LTP at temporommonic-CA1 synapses. *Learning Memory* **10,** 247–252 (2003).
17. Dvorak-Carbone, H. & Schuman, E. M. Patterned activity in stratum lacunosum moleculare inhibits CA1 pyramidal neuron firing. *J. Neurophys.* **82,** 3213–3222 (1999).
18. Dvorak-Carbone, H. & Schuman, E. M. Long-term depression of temporoammonic-CA1 hippocampal synaptic transmission. *J. Neurophys.* **81,** 1036–1044 (1999).
19. Otmakhova, N. A. & Lisman, J. E. Dopamine selectively inhibits the direct cortical pathway to the CA1 hippocampal region. *J. Neurosci.* **19,** 1437–1445 (1999).
20. El-Ghundi, M. *et al.* Spatial learning deficit in dopamine D1 receptor knockout mice. *Eur. J. Pharmacol.* **383,** 95–106 (1999).

21. Li, S., Cullen, W. K., Anwyl, R. & Rowan, M. J. Dopamine-dependent facilitation of LTP induction in hippocampal CA1 by exposure to spatial novelty. *Nature Neurosci.* **6,** 526–531 (2003).
22. Riedel, G. *et al.* Reversible neural inactivation reveals hippocampal participation in several memory process. *Nature Neurosci.* **2,** 898–905 (1999).
23. Frankland, P. W., O'Brien, C. O., Ohno, M., Kirkwood, A. & Silva, A. J. Alpha-CAMKII-dependent plasticity in the cortex is required for permanent memory. *Nature* **411,** 309–313 (2001).
24. Siapas, A. G. & Wilson, M. A. Coordinated interactions between hippocampal ripples and cortical spindles during slow-wave sleep. *Neuron* **21,** 1123–1128 (1998).
25. Sirota, A., Csicsvari, J., Bhul, D. & Buzsaki, G. Communication between neocortex and hippocampus during sleep in rodents. *Proc. Natl Acad. Sci. USA* **100,** 2065–2069 (2003).
26. Wilson, M. A. & McNaughton, B. L. Reactivation of hippocampal ensemble memories during sleep. *Science* **265,** 676–679 (1994).
27. Lee, A. K. & Wilson, M. A. Memory of sequential experience in the hippocampus during slow wave sleep. *Neuron* **36,** 1183–1194 (2002).

Supplementary Information accompanies the paper on **www.nature.com/nature**.

Acknowledgements We thank T. Siapas, G. Laurent, M. Sutton and other members of the Schuman laboratory for discussions. This work was supported by the Fundacao para a Ciencia e Technologia (FCT)—Portugal and the Howard Hughes Medical Institute.

Competing interests statement The authors declare that they have no competing financial interests.

Correspondence and requests for materials should be addressed to E.M S. (schumane@its.caltech.edu).

Enhanced virulence of influenza A viruses with the haemagglutinin of the 1918 pandemic virus

Darwyn Kobasa[1]*, Ayato Takada[2,3], Kyoko Shinya[2]*, Masato Hatta[1], Peter Halfmann[1], Steven Theriault[4], Hiroshi Suzuki[5], Hidekazu Nishimura[6], Keiko Mitamura[7]*, Norio Sugaya[7]*, Taichi Usui[8], Takeomi Murata[8], Yasuko Maeda[2], Shinji Watanabe[1], M. Suresh[1], Takashi Suzuki[3,9], Yasuo Suzuki[3,9], Heinz Feldmann[4] & Yoshihiro Kawaoka[1,2,3]

[1]*Department of Pathobiological Sciences, University of Wisconsin, Madison, Wisconsin 53706, USA*
[2]*Division of Virology, Department of Microbiology and Immunology, Institute of Medical Science, University of Tokyo, Tokyo 108-8639, Japan*
[3]*CREST, Japan Science and Technology Agency, Saitama, 332-0012, Japan*
[4]*Special Pathogens Program, National Microbiology Laboratory, Health Canada and Department of Medical Microbiology, University of Manitoba, Winnipeg, Manitoba R3E 3R2, Canada*
[5]*Department of Public Health, School of Medicine, Niigata University, Niigata, 951-8510, Japan*
[6]*Viral Research Center Clinical Research Division, Sendai National Hospital, Sendai, 983-8520, Japan*
[7]*Department of Pediatrics, Nippon Kokan Hospital, Kawasaki, 210-0852, Japan*
[8]*Department of Applied Biological Chemistry, Shizuoka University, Shizuoka 422-8529, Japan*
[9]*Department of Biochemistry, University of Shizuoka, School of Pharmaceutical Sciences and COE Program in the 21st Century, Yada, Shizuoka-shi 422-8526, Japan*

* Present addresses: National Microbiology Laboratory, Canadian Science Centre for Human and Animal Health, Winnipeg, Manitoba R3E 3R2, Canada (D.K.); Institute for Animal Experimentation, Tohoku University Graduate School of Medicine, Sendai 980-8575, Japan (K.S.); Department of Pediatrics, Kawasaki Municipal Hospital, Kawasaki 210-0013, Japan (K.M.); Department of Pediatrics, Keiyu Hospital, Yokohama 220-0012, Japan (N.S.)

The 'Spanish' influenza pandemic of 1918–19 was the most devastating outbreak of infectious disease in recorded history. At least 20 million people[1] died from their illness, which was characterized by an unusually severe and rapid clinical course. The complete sequencing of several genes of the 1918 influenza virus has made it possible to study the functions of the proteins encoded by these genes in viruses generated by reverse genetics, a technique that permits the generation of infectious viruses entirely from cloned complementary DNA. Thus, to identify properties of the 1918 pandemic influenza A strain that might be related to its extraordinary virulence, viruses were produced containing the viral haemagglutinin[2] (HA) and neuraminidase[3] (NA) genes of the 1918 strain. The HA of this strain supports the pathogenicity of a mouse-adapted virus in this animal[4,5]. Here we demonstrate that the HA of the 1918 virus confers enhanced pathogenicity in mice to recent human viruses that are otherwise non-pathogenic in this host. Moreover, these highly virulent recombinant viruses expressing the 1918 viral HA could infect the entire lung and induce high levels of macrophage-derived chemokines and cytokines, which resulted in infiltration of inflammatory cells and severe haemorrhage, hallmarks of the illness produced during the original pandemic[6].

The sequence of the HA receptor/fusion gene of the 1918 influenza A virus (H^{sp}) was determined in 1999 (ref. 2), followed shortly by the NA gene (N^{sp})[3], which codes for the viral sialidase. These molecules, which represent the major viral surface glycoproteins of influenza virus, are important targets of the host immune response, and critical changes in their structure can expand the viral host range and enhance the virulence of infection[7,8]. However, neither protein of the 1918 virus contains sequence motifs known to be associated with high virulence[2,3]. Attempts to account for the unusually high virulence of the virus have focused on the living conditions of soldiers, a highly susceptible group, and of civilians at the end of the First World War[9], as well as on potentially unique properties of the virus itself[10,11]. The combination of H^{sp} and N^{sp} in an A/WSN/33 (WSN) (H1N1) genetic background was shown to be pathogenic in mice without prior adaptation of the proteins to growth in these hosts[4,5], usually a prerequisite for producing a lethal infection in mice with a human virus. However, WSN itself is both adapted to and highly pathogenic in mice, so it was not possible to assess the possible contribution that H^{sp} and N^{sp} had made to the pathogenicity of the recombinant virus. Another candidate, the non-structural gene of the 1918 virus, had an attenuating effect when tested in a recombinant virus bearing the genetic background of A/Puerto Rico/8/34 (H1N1), also a highly pathogenic virus in mice[10]. Viruses generated with the matrix, nucleoprotein and non-structural protein genes of WSN replaced by the respective genes from the 1918 virus, together with H^{sp} and N^{sp}, were also pathogenic in mice[4,5] but not significantly more than the recombinant possessing only the H^{sp} and N^{sp} genes. Thus, the molecular basis for the unprecedented virulence of the 1918 pandemic virus remains uncertain, opening the way for studies that directly test the contribution of H^{sp} and N^{sp} to pathogenicity.

We therefore used reverse genetics[12] to produce a panel of recombinant viruses containing H^{sp} together with N^{sp} or the NA gene of A/Kawasaki/173/2001 (H1N1) (K173) in the background of the remaining negative-sense RNA gene segments derived from three influenza viruses: WSN, K173 and A/Memphis/8/88 (H3N2) (M88) (Table I). All recombinant viruses formed plaques on Madin–Darby canine kidney (MDCK) cell monolayers in the presence of trypsin and replicated efficiently to a high titre (data not shown).

To assess the contribution of H^{sp} and N^{sp} to pathogenicity *in vivo*, mice were intranasally inoculated with the recombinant and parental viruses. Each virus possessing H^{sp} as well as the WSN virus replicated to a high titre in the lungs by day 3 post-infection (p.i.; Table I) and was pathogenic, resulting in serious morbidity and eventually death. Notably, the K173 and M88 parental human viruses did not cause discernible morbidity in mice and replicated to only low titres in the lungs, whereas the K173/H^{sp} and M88/H^{sp} viruses, in which the original HA proteins were replaced with H^{sp}, caused lethal infection in mice. The N^{sp} protein did not contribute to viral pathogenicity, as viruses containing H^{sp} and N^{sp} were not